ACS OMEGA

http://pubs.acs.org/journal/acsodf

Article

# Proliferation and Metabolic Profiling of *Cynanchum wilfordii* Adventitious Roots Using Explants from Different Cultivation Methods

Hyejin Hyeon,[#] Eun Bi Jang,[#] Weon-Jong Yoon, Jong-Du Lee, Ho Bong Hyun, Yong-Hwan Jung, Jung Min, and Young-Min Ham*

Cite This: *ACS Omega* 2022, 7, 46756−46768

Read Online

ACCESS | Metrics & More | Article Recommendations | Supporting Information

**ABSTRACT:** *Cynanchum wilfordii* root is used in traditional herbal medicine owing to its various pharmacological activities. However, *C. wilfordii* roots are misused owing to their morphological similarities with *C. auriculatum*. Adventitious root (AR) culture can prevent such misuse, and the selection of plant materials is an important procedure for producing high-quality ARs. This study aimed to compare the proliferation and metabolic profiles of *C. wilfordii* ARs in two types of explants from different cultivation methods (either cultivated in open field (ECF) or cultivated on a heap of *C. wilfordii* (ECH)). After 4 weeks of culture, the proliferation rate and number and length of secondary ARs were determined, and 3/4 Murashige and Skoog (MS) salt medium, 4.92 $\mu$M indole-3-butyric acid (IBA), and 5% sucrose were suggested as the best proliferation conditions for ARs originating from both ECF and ECH. Through metabolic profiling, ARs from ECH were found to show higher accumulation patterns for flavonoids, polysaccharides, hydroxyacetophenones, aromatic amino acids, and mono-unsaturated fatty acids, which were ascribed to the activation of flavonoid biosynthesis, the phenylpropanoid pathway, and fatty acid desaturase, stimulated by abiotic stresses. In contrast, ARs from ECF had higher levels of TCA cycle intermediates, amino acids in the aspartate−glutamate pathway, and saturated and polyunsaturated fatty acids, indicating energy metabolism and plant development. Overall, the current study provided information on the optimal conditions for inducing *C. wilfordii* ARs with higher amounts of bioactive compounds.

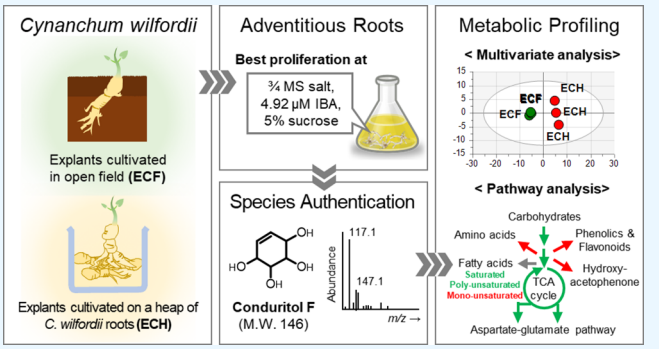


## INTRODUCTION

*Cynanchum wilfordii* (Maxim.) Hemsl. (family Asclepiadaceae) is a perennial vine, and its tubers, also called "Baeksuo," are grown for 2−3 years for subsequent use as herbs in oriental medicine.[1] A previous human clinical study has been demonstrated that *C. wilfordii* intake helps in maintaining healthy blood cholesterol levels.[2] Moreover, several *in vitro* and rodent *in vivo* studies have reported that *C. wilfordii* assists in bone disease prevention, protects hepatocytes, and prevents progression of aging.[3−5] *C. auriculatum* is another plant belonging to the Asclepiadaceae family and has morphological characteristics similar to those of *C. wilfordii*; however, it is not recognized as a food ingredient in Korea.[6] Based on a study that revealed an increased risk of miscarriage associated with *C. auriculatum* extract ingestion, the Korea Consumer Agency and the US Food and Drug Administration (FDA) have added it to the list of toxic plants, thereby prohibiting its use.[7] However, both the plants were named 'Baeksuo', which led to the availability of their mixture in the Korean herbal medicine market.[8] Mislabeling and misuse of *C. wilfordii* as *C. auriculatum*, to obtain economic benefits, has become a critical issue for consumers because it is directly linked to the quality and authenticity of herbal plants.

*In vitro* culture is a technology for culturing plant cells and tissues aseptically under artificial culture conditions, and it can stably produce specialized metabolites regardless of geographic or seasonal changes.[9] During *in vitro* culture of *C. wilfordii*, there is no risk of interference from *C. auriculatum*, since continuous culturing proceeds only after confirming that the explants belong to the original plant *C. wilfordii*.[10] Among the various *in vitro* culture techniques, adventitious root (AR) culture reportedly provides higher genetic and biochemical stability, along with higher contents of specialized metabolites, compared to callus culture.[11] Ahn et al. (2018) performed a

Received: September 8, 2022
Accepted: November 24, 2022
Published: December 8, 2022

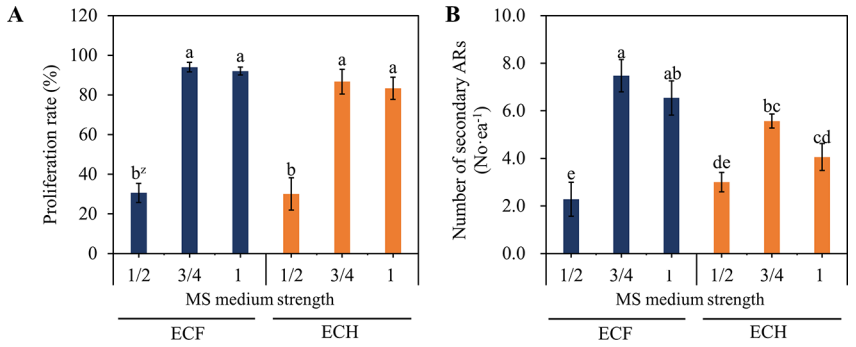


**Figure 1.** Characteristics of adventitious roots (ARs) derived from explants cultivated in an open field (ECF) and those cultivated on a heap of *C. wilfordii* roots (ECH) by MS salt concentration. Proliferation rate (A), number of secondary ARs (B). Basal medium: 4.92 $\mu$M IBA + 30 g/L sucrose + 2.4 g/L gelrite. [z]Different letters indicate significant differences at $p < 0.05$ according to Duncan's multiple range test ($n = 3$).

metabolite analysis of *C. wilfordii* roots in plants, cultivated *in vitro* and *ex vitro*, using FT-IR spectroscopy and found the overall metabolite pattern to be identical, indicating the possibility that *in vitro* cultured roots may be supplied as an herbal medicine instead of *ex vitro* plants.[10]

Various strategies have been implemented to increase the physiologically active metabolites in *in vitro* culture, including explant selection, finding a suitable medium composition, and elicitor treatment.[9,12,13] Among them, explant selection helps to establish better cell lines since the physiological activities of the cell lines become greater when they are derived from mother plants with high-yielding bioactive substances.[14] However, during plant growth of the same species, the production of bioactive compounds can be altered by exposure to different environmental conditions. For instance, a previous study had shown that antioxidant activity is significantly different between plant materials from artificial hydroponic cultivation and those from natural soil cultivation.[15] Using plant sources as cultivation substrates has been reported to cause a rapid change in flavonoid biosynthesis in cultured *Dendrobium officinale*.[16] For the above reasons, selection of proper cultivation methods for explants, for the efficient use of ARs as functional resources containing various specialized metabolites, is absolutely necessary.

Metabolomics provides a comprehensive identification of systematic chemical processes involving various metabolites in biological samples, such as plants, cells, and tissues.[17] All chemical constituents can be broadly divided into two groups, namely, primary and specialized metabolites.[18] Primary metabolites are essential for plant growth and development and are used as building blocks of specialized metabolites.[18] Specialized metabolites, such as pharmaceuticals, flavors, and fragrances, play important roles in environmental responses and are commercially used as biologically active compounds with great economic value.[19] Considering the increase in industrial demand for metabolites with health-promoting properties, metabolic profiling should be conducted to understand the interaction between primary and specialized metabolism and to find a way to regulate the levels of desired compounds in *C. wilfordii* ARs.

Although a previous study applied an *in vitro* culture technique to prevent misuse of *C. wilfordii* and to obtain stable and sufficient biomass ingredients, to the best of our knowledge, none of the studies have evaluated the optimal growth condition of ARs using different types of *C. wilfordii* explants, nor did they have conducted a comprehensive profiling of both primary and specialized metabolites.[10] Thus, the current study aimed to establish a medium composition suitable for the growth of *C. wilfordii* ARs, using explants derived from different cultivation methods, and to uncover the dynamic primary and specialized metabolism regulated by the abiotic factors of explants. Two types of plant materials were used in this experiment, namely, explants cultivated in an open field (ECF) and those cultivated on a heap of *C. wilfordii* (ECH). To identify the cultivation method of explants that would be better for the growth of ARs, primary and specialized metabolites (including amino acids, organic acids, sugars, fatty acids, hydroxyacetophenones, and phenolic compounds) were compared using high-performance liquid chromatography (HPLC) and gas chromatography−mass spectrometry (GC−MS). Species authentication of *C. wilfordii* ARs was performed by analyzing the chemical marker, conduritol F.

## RESULTS AND DISCUSSION

**Growth Characteristics of ARs Originating from ECF and ECH.** To identify the optimum concentration of minerals in the medium for the growth of *C. wilfordii* ARs induced by ECF and ECH, *C. wilfordii* ARs were cultured in three different concentrations of Murashige and Skoog (MS) salt (1/2, 3/4, and 1 strength).[20] Our study showed that both ECF and ECH produced higher proliferation rates in the 3/4 and 1 MS treatment groups than in the 1/2 MS treatment group ($p < 0.05$), and there was no significant difference between 3/4 and 1 MS concentrations in both ECF and ECH (Figure 1A). The number of secondary ARs was the highest in the 3/4 MS treatment group in both ECF and ECH types, and those were 3.3 and 1.9 times higher than in the 1/2 MS concentration, respectively. Considering the explant types, the overall number of secondary ARs from ECF was higher than that from ECH. In the 3/4 MS medium composition, the number of secondary ARs from ECF was 1.3 times higher than that from ECH (Figure 1B). In particular, browning started in the 1/2 MS medium after 3 weeks of culture, indicating that browning occurred faster than in the other media, when cultured for the same period (Figure S1). Inorganic salt concentration in the medium affects organogenesis and plant growth, and the MS medium contains a higher nitrogen content than other media.[13] In case of AR proliferation, the concentration of suitable inorganic salts varies depending on the plant. According to previous studies, *Echinacea angustifolia* ARs grow best at 1/2 MS concentration, whereas 1 MS was the optimal growth condition for *Pseudostellaria heterophylla* ARs.[21,22] In high-strength MS medium, low water potential affects the absorption of water and nutrients in the roots,


https://doi.org/10.1021/acsomega.2c05833
ACS Omega 2022, 7, 46756−46768

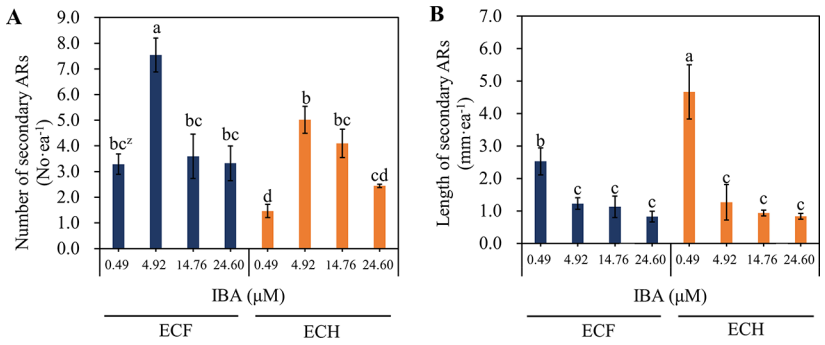


**Figure 2.** Effect of IBA concentration on the proliferation of *C. wilfordii* adventitious roots (ARs) derived from explants cultivated in an open field (ECF) and those cultivated on a heap of *C. wilfordii* roots (ECH). The number of secondary ARs (A), length of secondary ARs (B). Basal medium: 3/4 MS + 30 g/L sucrose + 2.4 g/L gelrite. [z]Different letters indicate significant differences at $p < 0.05$ according to Duncan's multiple range test ($n = 3$).

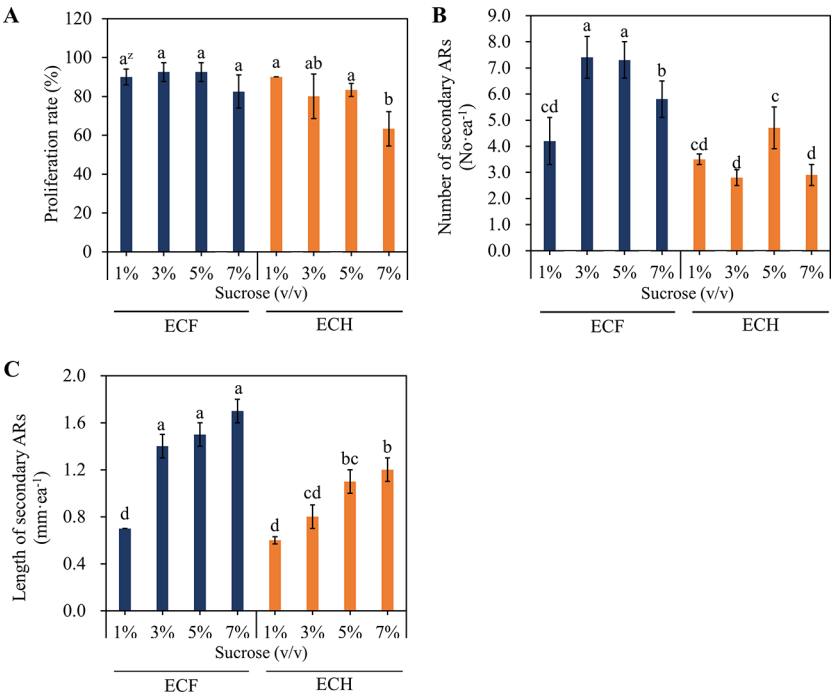


**Figure 3.** Characteristics of *C. wilfordii* adventitious roots (ARs) derived from explants cultivated in an open field (ECF) and those cultivated on a heap of *C. wilfordii* roots (ECH) by varying sucrose concentration. Proliferation rate (A), number of secondary ARs (B), and length of secondary ARs (C). Basal medium included 3/4 MS + 4.92 $\mu$M IBA + 2.4 g/L gelrite. [z]Different letters indicate significant difference at $p < 0.05$ according to Duncan's multiple range test ($n = 3$).

thereby reducing growth. In contrast, ARs grow rapidly in low-strength MS medium, although a lack of nutrients reduces the biomass levels.[23−25]

Indole-3-butyric acid (IBA) is another important factor for AR induction, since it initiates cell division and primordium formation, and induces cell dedifferentiation to form apical meristems.[26] The proliferation rate based on IBA concentration showed no significant difference, with a proliferation rate of 80% or more for both ECF and ECH (data not shown). The number of induced secondary ARs was the highest when both types were treated with 4.92 $\mu$M IBA, and the length of secondary ARs in ECF and ECH was the longest at 0.49 $\mu$M IBA (Figure 2). In *Hypericum perforatum*, secondary ARs were thin and long when treated with 2.46 $\mu$M IBA, but at a high concentration of 14.8 $\mu$M, the secondary ARs were shorter and thicker, similar to the results of this study.[27] Therefore, based on the number of secondary ARs and morphological observations of ARs of *C. wilfordii*, 4.92 $\mu$M IBA was considered optimal. Ahn et al. (2018) had reported the IBA concentration suitable for the proliferation of *C. wilfordii* ARs to be 24.60 $\mu$M, which differed from the results of this study.[10] A high concentration of exogenous IBA was not essential in this study, since the change in hormonal sensitivity was presumed to differ depending on the tissue, age, and developmental stage of the plant as well as the physiological conditions.[28]

After culturing for 4 weeks with different sucrose concentrations, the number of secondary ARs in ECF was the highest in 3% and 5% treatment groups (Figure 3B). In ECH, the number of secondary ARs was the highest at 5% sucrose, and proliferation was inhibited at 7% sucrose (Figure 3A,B). The optimal sucrose concentration differed between ECF and ECH, even though they originated from the same species. In plant culture, exogenous carbohydrates regulate


https://doi.org/10.1021/acsomega.2c05833
ACS Omega 2022, 7, 46756−46768

Table 1. Identification of Conduritol F in *C. Wilfordii* Adventitious Roots (ARs) from Explants Cultivated in an Open Field (ECF) and Those Cultivated on a Heap of *C. Wilfordii* Roots (ECH)

| compound | RT[a] (min) | RRT[b] (min) | mass fragment | quantification ion[c] | quantity (μg/mg)[d] | |
|---|---|---|---|---|---|---|
| | | | | | ECF | ECH |
| conduritol F-1 | 11.382 | 0.997 | 117, 147, 160 | 117 | 0.112 ± 0.008 | 0.048 ± 0.006 |
| conduritol F-2 | 11.463 | 1.004 | 117, 147, 160 | 117 | | |

[a]Retention time. [b]Relative retention time (retention time of analyte/retention time of internal standard). [c]Specific mass ion used for quantification. [d]Each value is the mean of three replicates ± standard deviation.

various physiological functions, including plant growth and metabolite synthesis, respiration, and osmotic pressure regulation, and maximal uptake of sucrose and other nutrients increases biomass and specialized metabolite content.[24,29] The type and concentration of sugar in apple root MM106 reportedly affects the rooting rate, number of roots, and root length.[30] Sucrose, the most commonly used carbon source, is used at a concentration range of 2−5% in most AR cultures. An increase in sucrose concentration within the appropriate range increases the AR biomass due to a decrease in the cell water content.[31] However, since high sucrose concentration reduces osmotic pressure, it can act as a stressor and directly stimulate the defense response, which can inhibit the growth of ARs, thereby affecting metabolite synthesis.[13,32]

**Analysis of Conduritol F as a Chemical Biomarker of *C. wilfordii*.** Development and enhancement of the culture system are crucial for the production of high-quality ARs. However, species authentication should primarily be conducted before the production of AR biomass to reduce indeterminacy in authentic *C. wilfordii* ARs. Previous studies had shown that conduritol F is a single biomarker that can be used to discriminate between *C. wilfordii* and *C. auriculatum*.[6,8] Thus, we analyzed conduritol F, which exists only in *C. wilfordii*, in ARs from ECF and ECH by GC−MS. Our results represented that conduritol F showed the formation of two derivatization products with characteristic fragment ions at *m/z* 117 $[M - 29]^+$, *m/z* 147 (base peak), and *m/z* 160 $[M + 14]^+$ (Table 1). Among these ions, $[M - 29]^+$ was the most dominant and corresponded to the loss of two methyl radicals in the molecule.[33] The precursor and product ions in the mass spectra of ribitol, used as an IS, agreed with those reported in the literature.[34] For accurate quantification, *m/z* 117 was selected for the analysis of conduritol F, and *m/z* 147 was selected for the IS. In the quantification of conduritol F in *C. wilfordii* ARs, a significantly higher level of conduritol F was detected in ECF types (0.112 ± 0.008 μg/mg) than in ECH types (0.048 ± 0.006 μg/mg) (Table 1). Our results confirmed that the two AR samples were cultured from genuine *C. wilfordii* root. Additionally, the results suggested that metabolites could be produced differently depending on the properties of the initial explants.

**Multivariate Analysis.** Generally, specialized metabolites, such as hydroxyacetophenones and phenolic compounds, are important for *C. wilfordii* in view of their extensive biological activities, including antioxidant, anti-inflammatory, neuroprotective, and anti-tumor activities.[35,36] Primary metabolites, such as amino acids, organic acids, sugars, and fatty acids, affect the biosynthesis of various specialized metabolites as precursors.[37] For these reasons, both primary and specialized metabolites were analyzed in the present study. We identified 54 metabolites, including conduritol F (Figure S2), hydroxyacetophenones (Figure S3, Table S1), phenolic compounds (Figure S4, Table S2), low-molecular-weight hydrophilic compounds (Figure S5, Table S3), and fatty acids (Figure S6, Table S4).

Multivariate analysis is an approach for measuring several biologically relevant features in a large-scale metabolome dataset, with two of the most popular methods being principal component analysis (PCA) and partial least-squares discriminant analysis (PLS-DA). PCA provides an informative first look at group structures with unbiased dimensionality reduction.[38] Thus, PCA was initially applied to conceptualize the overall patterns in metabolite composition between ARs from ECF and ECH. In the score plot, the two highest-ranking principal components accounted for 85.1% of the total variance in the dataset. Principal component 1 (PC1), accounting for 68.8% of the total variance, resolved a clear separation between ARs from ECF and those from ECH (Figure 4A). The corresponding loading plot enabled the identification of several metabolites that contributed to the separation between the two groups (Figure 4B). In the loading plot, positive PC1 values were mainly attributable to major phenolic compounds, amino acids, and hydroxyacetophenones, which implied that these metabolites were more abundant in ARs from ECH than in those from ECF. The notable metabolites with positive values for PC1 were rutin, phenylalanine, and 4′-hydroxyacetophenone with eigenvector values of 0.1606, 0.1611, and 0.1374, respectively. On the other hand, negative PC1 values were ascribable to most organic acids and polyunsaturated fatty acids, which indicated that the levels of these compounds were higher in ARs from ECF than in those from ECH. The representative metabolites with negative values for PC1 were citric acid and linolenic acid, with eigenvector values of −0.1621 and −0.1609, respectively. The results agreed with previous results in the fact that the types of explants used for AR induction influenced the accumulation of various phytochemicals differently due to their endogenous and exogenous factors.[39,40]

Compared to PCA, which preserves information regarding class groups, PLS-DA is a chemometric technique used to maximize the separation between different groups of samples and is more accurate in measuring significant metabolites.[41] To further explore the novel metabolic differences between the two AR types, PLS-DA was performed (Figure 5A). In this experiment, PLS-DA score plots showed clear separation by explant origin. To estimate the quality of the PLS-DA model, we calculated the two quality parameters, goodness of fit ($R^2$) and goodness of prediction ($Q^2$). Generally, $R^2$ values closer to 1 are considered to represent a good description of the data by the PLS-DA model, and $Q^2$ values higher than 0.9 are considered to represent excellent predictability.[42] We obtained an $R^2_Y$ of 0.997 and $Q^2$ of 0.985 by validation analysis using PLS-DA. This implied that PLS-DA significantly contributed to the separation of the two types of ARs, with high goodness of fit and prediction. Variable importance in projection (VIP) plots were used to examine the significant features responsible


https://doi.org/10.1021/acsomega.2c05833
ACS Omega 2022, 7, 46756−46768

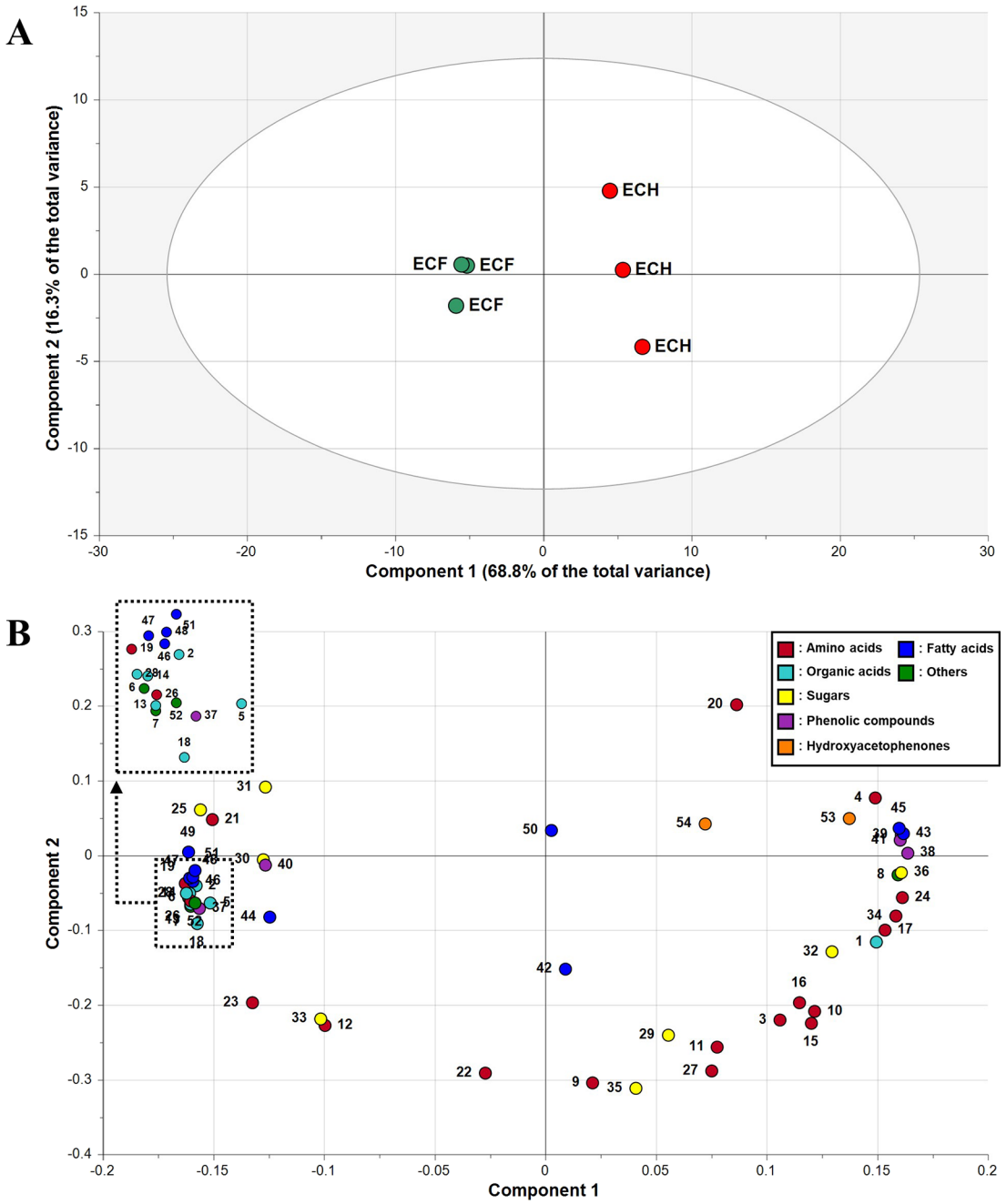


**Figure 4.** Score (A) and loading (B) plots of principal components 1 and 2 from the principal component analysis results obtained from conduritol F, hydroxyacetophenones, phenolic compounds, low-molecular-weight hydrophilic compounds, and fatty acids data for *C. wilfordii* adventitious roots (ARs) derived from explants cultivated in an open field (ECF) and those cultivated on a heap of *C. wilfordii* roots (ECH). Plot annotation: 1, lactic acid; 2, glycolic acid; 3, alanine; 4, valine; 5, urea; 6, ethanolamine; 7, glycerol; 8, phosphoric acid; 9, leucine; 10, isoleucine; 11, proline; 12, glycine; 13, succinic acid; 14, fumaric acid; 15, serine; 16, threonine; 17, *β*-alanine; 18, malic acid; 19, aspartic acid; 20, methionine; 21, pyroglutamic acid; 22, GABA; 23, glutamic acid; 24, phenylalanine; 25, xylose; 26, asparagine; 27, glutamine; 28, citric acid; 29, fructose; 30, mannose; 31, galactose; 32, glucose; 33, inositol; 34, tryptophan; 35, sucrose; 36, raffinose; 37, caffeic acid; 38, epicatechin; 39, rutin; 40, benzoic acid; 41, kaempferol; 42, C16:0; 43, C16:1; 44, C18:0; 45, C18:1; 46, C18:2; 47, C18:3; 48, C20:0; 49, C22:0; 50, C22:1; 51, C24:0; 52, conduritol F; 53, 4'-hydroxyacetophenone; 54, 2′,4'-dihydroxyacetophenone.

for *C. wilfordii* AR differentiation (Figure 5B). VIP scores higher than 1 strongly contributed to sample differentiation.[43] In this study, a total of 33 metabolites, including amino acids, organic acids, fatty acids, and phenolic compounds, were included in the group with VIP values greater than 1, underlining their importance in discriminating *C. wilfordii* ARs between ECF and ECH. The outcomes were consistent with the PCA results. In particular, the significant importance of most of the phenolic compounds (except benzoic acid) and 4′-hydroxyacetophenone was notable, since the phenolic compounds and 4′-hydroxyacetophenone exhibit medicinal activity and efficacy of *C. wilfordii* ARs as bioactive compounds.[35,36]

**Metabolites−Metabolites Correlations.** To investigate the relationships across metabolites of *C. wilfordii* ARs involved in closely related metabolic pathways, we performed Pearson's


https://doi.org/10.1021/acsomega.2c05833
ACS Omega 2022, 7, 46756−46768

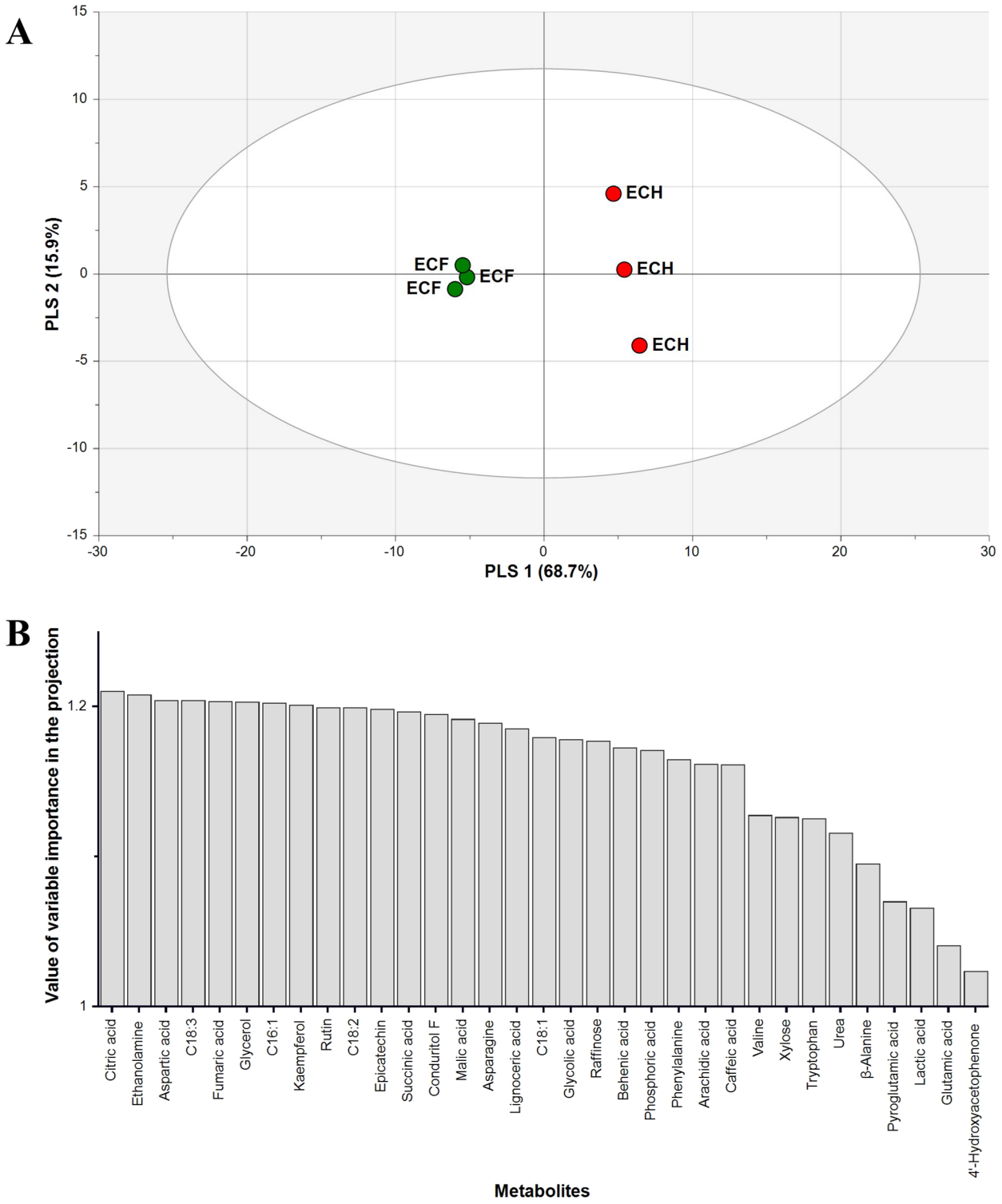


**Figure 5.** Partial least squares-discriminant analysis (PLS-DA) score plots (A) and variable importance in projection (VIP) score above 1 (B) for conduritol F, hydroxyacetophenones, phenolic compounds, low-molecular-weight hydrophilic compounds, and fatty acids data for *C. wilfordii* adventitious roots (ARs) derived from explants cultivated in an open field (ECF) and those cultivated on a heap of *C. wilfordii* roots (ECH).

correlation and hierarchical cluster analyses (HCA). Two major composition clusters have been described by HCA (Figure 6, boxed within dotted lines). In the first group, positive correlations were observed between organic acids and five amino acids (glutamic acid, aspartic acid, asparagine, glycine, and pyroglutamic acid), which belong to the TCA cycle and nitrogen metabolism into amino acids. For example, aspartic acid was positively correlated with citric acid ($r$ = 0.9957, $p$ < 0.001), malic acid ($r$ = 0.9800, $p$ < 0.001), and succinic acid ($r$ = 0.9928, $p$ < 0.001). Furthermore, all saturated and polyunsaturated fatty acids, except C16:0, were strongly correlated with organic acids and amino acids. Significant correlations between the compounds participating in the TCA cycle, nitrogen metabolism, and fatty acid


https://doi.org/10.1021/acsomega.2c05833
ACS Omega 2022, 7, 46756−46768

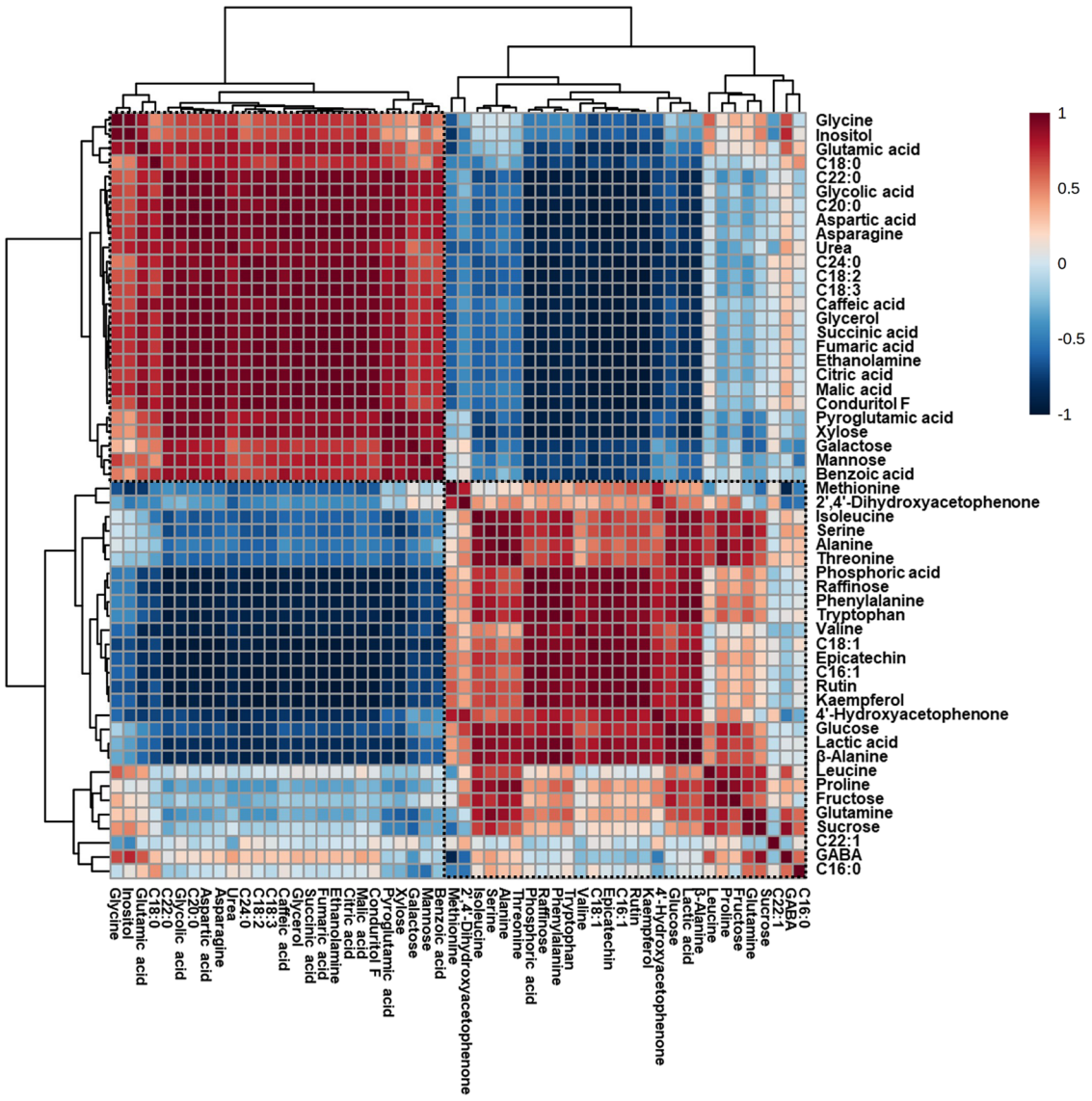


**Figure 6.** Correlation matrix for conduritol F, hydroxyacetophenones, phenolic compounds, low-molecular-weight hydrophilic compounds, and fatty acids data for *C. wilfordii* adventitious roots (ARs) derived from explants cultivated in open field (ECF) and those cultivated on a heap of *C. wilfordii* roots (ECH). Each square indicates the Pearson's correlation coefficient of a pair of compounds, with the value of this coefficient represented by the intensity of blue or red color, indicated on the color scale.

metabolism were associated with the modulation of energy metabolism.[44] Our findings were in agreement with the previous reports that revealed energy generation to be activated by the release of TCA cycle intermediates, aspartate−glutamate pathway, and fatty acids under regular growth conditions.[45,46]

The second group mainly comprised phenolic compounds, polysaccharides, aromatic amino acids, hydroxyacetophenones, and mono-unsaturated fatty acids, some of which are involved in phenylpropanoid and flavonoid biosynthesis. For instance, raffinose was significantly correlated with phenolic compounds, including epicatechin ($r$ = 0.9717, $p$ < 0.01), rutin ($r$ = 0.9370, $p$ < 0.01), and kaempferol ($r$ = 0.9605, $p$ < 0.01), as well as with aromatic amino acids, including phenylalanine ($r$ = 0.9851, $p$ < 0.001) and tryptophan ($r$ = 0.9672, $p$ < 0.01). The strong correlations across raffinose, flavonoids, and aromatic amino acids were in agreement with a previous report by Kim et al. (2021).[47] However, this study also revealed that phenolic compounds were highly correlated with hydroxyacetophenones and mono-unsaturated fatty acids. For example, epicatechin was positively correlated with 4′-hydroxyacetophenone ($r$ = 0.8636, $p$ < 0.05), C16:1 ($r$ = 0.9794, $p$ < 0.001), and C18:1 ($r$ = 0.9706, $p$ < 0.01). The result indicated positive interactions among phenolic compounds, hydroxyacetophenones, and mono-unsaturated fatty acids, as supported by previous studies. Zhu et al. (2018) had reported that the concentration of aromatic compounds, such as ferulic acids and vanillin, were accelerated together with those of 4′-hydroxyacetophenone by the degradation of lignin in plant cell walls.[48] O'Brien et al. (2012) also noted that hydroxyacetophenones as well as other phenolic compounds are utilized to reduce reactive oxygen species (ROS) during defense mechanisms.[49] Moreover, the concentrations of mono-unsaturated fatty acids, including C16:1 and C18:1, were increased under stress conditions, and the compounds could be the key to reducing the burst of ROS.[50,51] Overall, our results largely supported the positive relationship across hydroxyacetophenones, mono-unsaturated


https://doi.org/10.1021/acsomega.2c05833
ACS Omega 2022, 7, 46756−46768

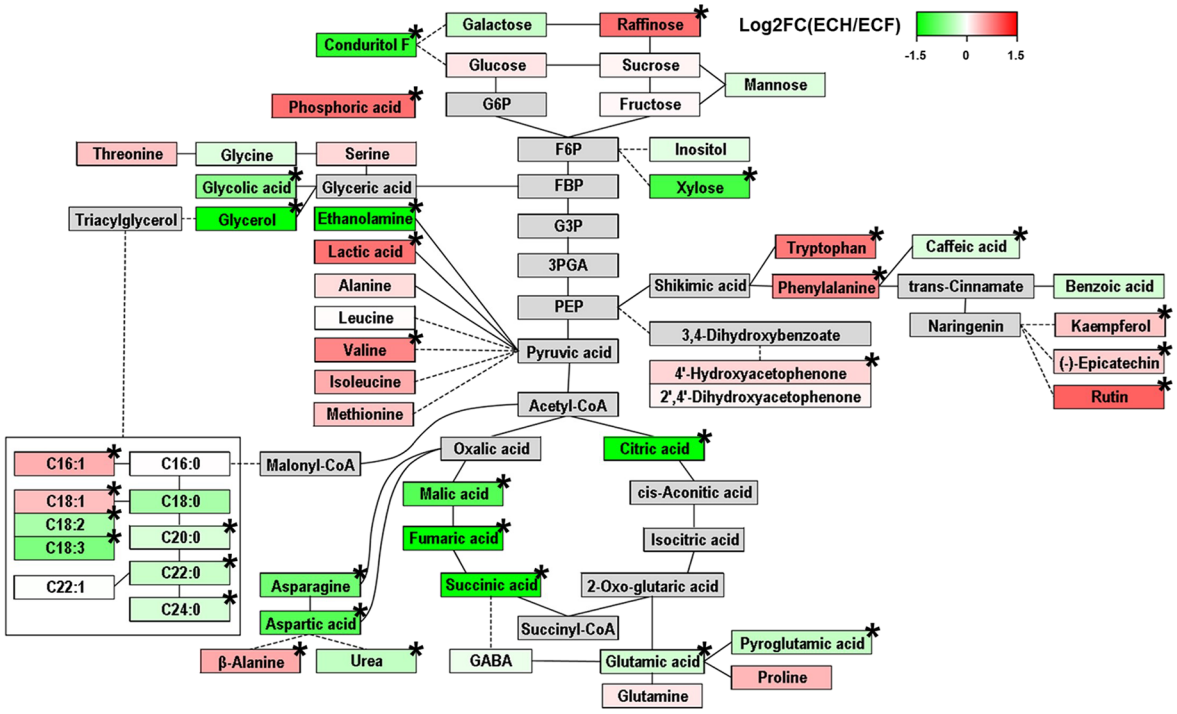


**Figure 7.** Metabolic pathway diagrams of *C. wilfordii* adventitious roots (ARs) derived from explants cultivated in an open field (ECF) and those cultivated on a heap of *C. wilfordii* roots (ECH). The expression data consist of $\log_2$-transformed fold change (FC) values ($\log_2$FC). A $\log_2$FC value range is $-1.5 < \log_2 FC < 1.5$. If $\log_2$FC value is higher than zero (indicated in red), metabolite content would be higher in ARs from ECH than in those from ECF. If $\log_2$FC value is less than zero (indicated in green), metabolite content would be lower in ARs from ECH. If $\log_2$FC value is zero (indicated in white), metabolite content would be identical in both types of AR. Significant differences between ARs induced from ECF and ECH were identified by the *t* test ($^*p < 0.05$).

fatty acids, and phenolic compounds to improve stress tolerance.

**Metabolic Pathway Analysis.** Based on multivariate analysis results using PCA, PLS-DA, and HCA, metabolic differences between the two ARs from ECH and ECF were notable, and the differences were closely related to metabolic pathways. To systematically compare the metabolites involved in adaptation to different growth conditions, metabolic pathway maps were drawn using PathVisio, and significant metabolites with VIP values greater than 1.0 and *p* values less than 0.05 were indicated by asterisks (*) (Figure 7). Abundance of metabolites in the ARs from ECH and ECF was visualized using red and green color gradients, respectively.

Regarding flavonoid biosynthesis and the phenylpropanoid pathway, our results showed the levels of flavonoids (rutin, epicatechin, and kaempferol) and aromatic amino acids (phenylalanine and tryptophan) to be higher in the ARs from ECH. Plants have various tolerance mechanisms for survival under environmental conditions. In addition, major metabolites induced by environmental stress usually exhibit antioxidant activity.[52] Zhang et al. (2017) had reported that adverse environmental conditions lead to the expression of genes encoding enzymes involved in the accumulation of rutin, a major flavonoid in tartary buckwheat, thereby improving abiotic stress resistance as an antioxidant.[53] Similarly, kaempferol and epicatechin have been reported to protect plant cells as *in vitro* ROS scavengers under environmental stress conditions in *Arabidopsis thaliana*.[54,55] Further, the synthetic pathway of aromatic amino acids has been reported to be consecutively upregulated owing to the higher levels of flavonoids required for antioxidant activities.[44,56] Thus, we suggested that the increase in rutin, epicatechin, and kaempferol contents could be associated with the stress response metabolism of mother plants against the heap-cultivation conditions. Moreover, our metabolic pathway results indicated the accumulation of these flavonoids to be manipulated by the enhanced production of phenylalanine and tryptophan, which are components of the phenylpropanoid pathway.

With regard to sugar metabolism, most sugar compounds did not show prominent changes. However, we confirmed that ARs from ECH, exposed to harsh environmental conditions, had higher amounts of raffinose. Raffinose is an abiotic stress-responsive metabolite with osmoprotective properties.[57] A myriad of abiotic stresses stimulate genes and enzymes related to the activation of raffinose synthase.[58] On the other hand, the content of xylose showed a prominent decrease in ARs from ECH. Xylose is a known precursor of hemicellulose in the plant cell walls.[59] Napoleão et al. (2017) observed hemicellulose biosynthesis and a reduction in xylose content in *Brachypodium distachyon* stems after treatment with methyl jasmonate, which induces plant defense responses.[60] Therefore, we proposed that the heap cultivation method increases the accumulation of raffinose and reduces the content of xylose to protect *C. wilfordii* mother plants that are exposed to abiotic stresses.

In the TCA cycle and nitrogen metabolism, the amounts of organic acids (citric acid, succinic acid, fumaric acid, malic acid, and urea) and amino acids in the aspartate−glutamate pathway (aspartic acid, asparagine, glutamic acid, and pyroglutamic acid) were significantly higher in the ARs from ECF than in those from ECH. The TCA cycle is usually


https://doi.org/10.1021/acsomega.2c05833
ACS Omega 2022, 7, 46756−46768

activated to generate energy and promote plant development in favored modes of cultivation.[44] As a consecutive enhancement of organic acid content, the synthetic pathway of amino acids could be upregulated by supplying carbon skeletons.[61] Thus, ARs from ECF, which spent time in non-stress conditions during the growth of mother plants, were expected to contain higher concentrations of aspartic acid, asparagine, glutamic acid, and pyroglutamic acid through activation of the TCA cycle. However, other amino acids, including valine and $\beta$-alanine, were largely accumulated in ARs from ECH. This was because amino acids in the aspartate−glutamate pathway are commonly used as nitrogen carriers and are converted into other amino acids, such as valine, threonine, and isoleucine.[62] We speculated that the large amount of amino acids in the aspartate−glutamate pathway was consumed for adaptation to the heap-cultivation conditions, resulting in the utilization of these amino acids for the synthesis of other amino acids, such as valine and $\beta$-alanine.

With regard to fatty acid metabolism, the present study showed that the levels of mono-unsaturated fatty acids were higher in ARs from ECH, whereas those of saturated and polyunsaturated fatty acids were higher in ARs from ECF. The change in the levels of saturated and unsaturated fatty acids was found to protect plant cells from multiple environmental stresses. Analysis of tobacco plants exposed to chilling stress showed a significant decrease in 16- and 18-carbon saturated fatty acid levels and expression of fatty acid desaturase genes.[63] In soybean leaves, salt resistance showed a decreased ratio of C18:2 and C18:3 to C18:1, representing the association of fatty acid composition with stress responses.[64] In addition, exposure of pepper seedlings to metal stress resulted in the reduction of polyunsaturated fatty acids, activating efficient defense mechanisms against ROS.[65] Likewise, in the present study, the comparatively low content of saturated fatty acids in ARs from ECH might be initiated by fatty acid desaturase. Subsequently, synthesis of mono-unsaturated fatty acids was enhanced and levels of polyunsaturated fatty acids were reduced in *C. wilfordii* explants under heap cultivation to support plant defense against abiotic stresses.

## CONCLUSIONS

The objective of this study was to examine the optimal medium composition for the growth of *C. wilfordii* ARs and the content of central primary and bioactive specialized metabolites for the efficient selection of mother plants. The study found that 3/4 MS salt medium, 4.92 $\mu$M IBA, and 5% sucrose were the best for the proliferation of both ARs originating from ECH and ECF. Before metabolic profiling, authenticity of the AR species was confirmed by analyzing conduritol F, a chemical marker of *C. wilfordii*. Multivariate analysis showed the metabolite differences and correlations to be derived from common or closely related pathways related to abiotic stress. ARs from ECH featured higher levels of phenolic compounds, polysaccharides, aromatic amino acids, hydroxyacetophenones, and mono-unsaturated fatty acids, which were associated with various mechanisms to protect the mother plants from abiotic stresses. In contrast, ARs from ECF had higher levels of TCA intermediates, amino acids in the aspartate−glutamate pathway, and saturated and polyunsaturated fatty acids, most of which were related to energy metabolism and plant development. Our results suggested that ECH is a better line for the production of valuable specialized metabolites that participate in the biosynthesis of flavonoids and hydroxyacetophenones, including rutin, epicatechin, kaempferol, and 4′-hydroxyacetophenone. The results suggested that using plants of the same species as substrates can be a new strategy to increase the content of functional specialized metabolites. Our study might help in selecting optimal explants for the induction of ARs with high contents of bioactive metabolites. Future study will focus on additional scale-up and *in vitro* screening studies to expand the possibility of *C. wilfordii* ARs in industrial use, along with various functional characteristics.

## METHODS

**Plant Materials and AR Induction.** *C. wilfordii* root, provided by Jeju Chyeonnyeonyakcho Farming Co. (Aewol-eup, Jeju Island, Korea), was used as the raw material, and two methods of cultivation of mother plants were used for the induction of ARs. One method was initiated from explants cultivated in an open field for 3 years. The other method was initiated from explants cultivated on a heap of *C. wilfordii* roots for 6 months, after cultivation in an open field for 2 years and 6 months. The workflow designed in this experiment is shown in Figure S7. For surface sterilization, explants were soaked in 70% ethanol for 1 min, rinsed with sterile deionized water, and immersed in a 2% (v/v) sodium hypochlorite solution supplemented with 1−2 drops of Tween-20 for 20 min. After rinsing thrice with sterile deionized water, explants were cultured in MS medium supplemented with 4.92 $\mu$M IBA, 30 g/L sucrose, and 2.4 g/L gelrite at 24 ± 1 °C under dark conditions. Explants (0.5 cm) were cut and placed in the medium.

**Proliferation of *C. wilfordii* ARs.** To obtain a medium composition suitable for the growth of ARs, MS salt (1/2, 3/4, and 1 strength), IBA (0.49, 4.92, 14.76, and 24.60 $\mu$M), and sucrose (1, 3, 5, and 7% (v/v)) concentrations were varied and culture was performed for 4 weeks. pH of all media was adjusted to 5.8 ± 1 before autoclaving, and then the media were sterilized at 121 °C and 1.2 atm for 15 min. The experiments were performed with one factor at a time, and the ARs were randomly placed. After 4 weeks of culture, the proliferation rate and number and length of the secondary ARs were recorded. Proliferation rate was measured as the ratio of the explants induced from the secondary ARs induced of 10 explants. Number and length of secondary ARs are the average of those derived from each explant. For metabolic comparison of ARs originating from ECF and ECH, 0.1 g (fresh weight) of ARs was inoculated in 100 mL medium containing 3/4 MS, 4.92 $\mu$M IBA, and 3% sucrose, cultured with shaking at 100 rpm for 4 weeks, washed with deionized water, and eventually freeze-dried at −85 °C.

**Analysis of Conduritol F with GC−MS.** To identify conduritol F in *C. wilfordii* ARs, samples were extracted and derivatized using previously reported methods with some modifications.[66,67] Each 50 mg of lyophilized sample was dissolved in 1 mL of methanol:water:chloroform 2.5:1:1 (v/v/v) solution, and ribitol (60 $\mu$L, 200 $\mu$g/mL in methanol) was introduced as an internal standard (IS). After incubation at 37 °C for 30 min, the samples were centrifuged at 13,000 rpm for 3 min. The polar phases (800 $\mu$L) were transferred to fresh tubes, mixed with water (400 $\mu$L), and centrifuged under identical conditions as above. The upper layers (900 $\mu$L) were pipetted into new tubes and concentrated for 3 h. The remaining residues were freeze-dried at −85 °C for 18 h. For derivatization, 80 $\mu$L of 2% methoxyamine hydrochloride (MOX) in pyridine (v/v) was added and incubated at 30 °C


https://doi.org/10.1021/acsomega.2c05833
ACS Omega 2022, 7, 46756−46768

for 90 min. Next, 80 μL of *N*-methyl-*N*-(trimethylsilyl) trifluoroacetamide (MSTFA) was added and incubated again at 37 °C for 30 min. The derivatized samples were analyzed on an Agilent 7890A GC (Agilent, Palo Alto, CA, USA) equipped with an Agilent 5975C MS and separated on a CP-Sil 8CB low-bleed/MS fused-silica capillary column (30 m × 0.25 mm i.d. × 0.25 μm film thickness; Agilent). For each run, 1 μL of sample was injected using a split ratio of 25:1. Helium was used as the carrier gas, flowing at a constant rate of 1.00 mL/min. The injection, MS quadrupole, and ion source temperatures were 230, 150, and 230 °C, respectively. The oven temperature program was initially set at 80 °C for 2 min, ramped to 320 °C at 15 °C/min, and was finally held at 320 °C for 10 min. The ionization voltage was set at 70 eV. The mass spectrum of each compound was acquired for *m/z* 85−600, and *m/z* 117 and *m/z* 147 were detected in the selected ion monitoring (SIM) acquisition mode. Qualification of conduritol F was conducted by direct comparison of retention time and mass spectra with those of commercially available standards acquired by methoxime derivatization and trimethylsilyl etherification procedures. For absolute quantification, an accurate calibration curve was prepared by loading conduritol F in the range of 2.5−30 μg with fixation of the IS at 12 μg. Chromatographic data were processed using ChemStation (Agilent) software.

**Analysis of Hydroxyacetophenones by HPLC.** Hydroxyacetophenones were extracted and analyzed according to previously described procedures with slight modifications.[8] For extraction of hydroxyacetophenones, 2 g of each AR sample was mixed with 70% ethanol (40 mL) for 24 h. Solvent residues were filtered through a filter paper (No. 2; Advantec, Tokyo, Japan). After evaporation, the extracted solvents were lyophilized under vacuum in a freeze-dryer (FD8512; IlShinBioBase, Dongducheon, Korea). Hydroxyacetophenones were analyzed from 10 mg of 70% ethanol extracts, which were mixed with 1 mL of 70% methanol, sonicated for 1 h, and centrifuged at 13,000 rpm for 10 min. The supernatants were filtered using a 0.50 μm PTFE filter (Advantec) into amber glass vials with a screw cap. The sample extracts were analyzed using a Thermo U3000 HPLC system (Thermo Fisher Scientific, Waltham, MA, USA) equipped with a DAD-3000 UV−vis detector (Thermo Fisher Scientific). The dissolved sample extract (10 μL) was loaded into a Cadenza CD-C18 column (150 × 4.6 mm, 3 μm particle size; Imtakt Corp., Kyoto, Japan). The flow rate was set to 1 mL/min, and the column temperature was maintained at 40 °C. Mobile phases A and B comprised 0.5% acetic acid in water and acetonitrile, respectively. The gradient program used was as follows: 0 min−20% B; 2 min−20% B; 20 min−30% B; 21 min−70% B; 26 min−100% B; 27 min−20% B; 42 min−20% B. The chromatogram was recorded at 200−400 nm, and peaks were obtained at 270 nm. The retention times and UV absorption spectra of each hydroxyacetophenone were compared to those of the standards. The amount of each compound was calculated from the calibration curve constructed by plotting the concentrations of standards ranging from 1.25 to 50 μg/mL. The resultant data were processed using Chromeleon 7 software (Thermo Fisher Scientific).

**Analysis of Phenolic Compounds with HPLC.** Extraction and analysis of phenolic compounds were performed according to a previously published method, with some modifications.[68] For each sample, 100 mg of lyophilized powder was extracted with 1 mL of methanol and 200 μL of 0.1 M hydrochloric acid (HCl). After sonication for 1 h, samples were centrifuged at 13,000 rpm for 10 min. The upper layer (900 μL) was transferred to a fresh tube, and the remaining pellet was re-extracted with methanol (1 mL). Following sonication and centrifugation under conditions similar to those described above, the upper layer was collected and concentrated using a centrifugal evaporator (CVE-3000, EYELA, Tokyo, Japan). The resulting extract was dissolved in methanol (1 mL) and filtered through a 0.50 μm syringe filter (Advantec). The obtained compounds were analyzed using a Waters Alliance e2695 HPLC system (Waters Corp., Milford, MA, USA) equipped with a photodiode array detector set at 280 nm. The dissolved sample extract (20 μL) was separated using a Zorbax CB-C18 column (250 × 4.6 mm, 5 μm particle size; Agilent). The flow rate and column temperature were set at 1 mL/min and 40 °C, respectively. The mobile phase solvent A was 0.1% acetic acid in water and solvent B was 0.1% acetic acid in acetonitrile. Composition of the mobile phase was programmed as follows: 0 min−8% B; 2 min−10% B; 35 min−30% B; 50 min−90% B; 51 min−100% B; 60 min−100% B; 63 min−8% B; wavelengths were monitored in the range of 200−400 nm, and the peak was obtained at 280 nm. Peak identification was performed by comparing the retention times and UV absorption spectra with those of the standards. Quantitative analysis of phenolic compounds was done using external calibration curves with concentrations ranging from 2.5 to 80 μg/mL. Data acquisition was performed using the Empower 3 software (Waters Corporation).

**Analysis of Low-Molecular-Weight Hydrophilic Compounds with GC−MS.** For the analysis of low-molecular-weight hydrophilic compounds, the methods for sample extraction, derivatization, GC−MS operation, and oven temperature programming were adopted from the protocol employed for conduritol F analysis. Mass spectra were acquired in scan mode over a mass range of 85−600 *m/z*. In-house and NIST libraries were used to identify the metabolites, and the identities were confirmed using commercial standards. Quantitative calculation was conducted based on the ratio of the peak area of the analyte to that of the IS.

**Analysis of Fatty Acids with GC−MS.** The extraction method used for fatty acids was described previously.[44] Briefly, 100 mg of lyophilized samples was weighed, and 2.5 mL of chloroform:methanol (2:1, v/v) solution was added. Pentadecanoic acid (200 μL, 1 mg/mL in chloroform) was added to the mixture as the IS. All the samples were vortexed and placed in a sonicator for 20 min. Next, 2.5 mL of sodium chloride solution (0.58% w/v) was added to the sample mixtures and centrifuged at 4000 rpm at 4 °C for 10 min. After pipetting the bottom layers into new tubes, the contents were evaporated using a centrifugal evaporator (EYELA) for 1 h. Methanol (180 μL), toluene (100 μL), and 5 M sodium hydroxide (20 μL) were introduced to the concentrated samples and incubated at 85 °C for 5 min. Methylation was activated by the addition of 14% (w/v) boron trifluoride followed by incubation under the same conditions described above. Water (400 μL) and pentane (800 μL) were then added to the samples. After centrifugation at 13,000 rpm for 15 min, the upper layers were collected in new tubes and concentrated for 30 min. The resulting extract was dissolved in hexane (200 μL) and filtered through a 0.50 μm syringe filter (Advantec). Samples were analyzed using an Agilent 7890A GC coupled with an Agilent 5975C MS. For each run, 1 μL of sample was injected into an HP-5MS column (30 m × 0.25 mm i.d. × 0.25


https://doi.org/10.1021/acsomega.2c05833
ACS Omega 2022, 7, 46756−46768

μm film thickness; Agilent) with a split ratio of 25:1. Helium gas was passed through the column at a flow rate of 1.00 mL/min. The injection, MS quadrupole, and ion source temperatures were set at 280, 150, and 230 °C, respectively. The oven temperature was initially maintained at 100 °C for 3 min and subsequently ramped to 180 °C at a rate of 15 °C/min. Subsequently, the temperature was increased to 250 °C at 5 °C/min and maintained for 3 min. The temperature was finally increased to 320 °C at a rate of 20 °C/min and maintained for 12 min. The mass range was set from 85 to 600 *m/z*, and ions were detected in SIM acquisition mode for peak analysis. Ionization voltage was set at 70 eV. Qualitative and quantitative analyses of fatty acids were performed using standards and a fatty acid methyl ester (FAME) mixture (C8−C24). Chromatographic data were obtained using ChemStation (Agilent) software.

**Statistical Analysis.** For statistical analysis of the growth characteristics of ARs, one-way analysis of variance (ANOVA) was performed using Statistical Analysis System (SAS) software (version 9.4; SAS Institute Inc., Cary, NC, USA). Statistical assessments of the differences across mean values were performed using Duncan's multiple range test. For the metabolic comparison of ARs originating from ECF and ECH, all data were normalized with unit-variance scaling and then applied to PCA and PLS-DA using soft independent modeling of class analogy (SIMCA) software (version 17.0; Umetrics, Umeå, Sweden). HCA and Pearson's correlation analyses were performed using MetaboAnalyst 5.0 (www.metaboanalyst.ca) to confirm metabolite−metabolite correlations. For metabolite mapping, fold changes (FCs) were calculated by dividing the average data of ARs from ECH by those of ARs from ECF and then transformed into $\log_2$ values. PathVisio software (version 3.3.0, http://www.pathvisio.org, Maastricht University, Maastricht, The Netherlands) was used to link $\log_2$-transformed values with the metabolic pathways drawn based on the *Arabidopsis thaliana* pathway in WikiPathways, reference pathway in the KEGG database, and the previously published literature.[48,69] Using GraphPad Prism 8 (San Diego, CA, USA), independent Student's *t* tests were conducted to represent significantly different metabolites with $p < 0.05$ as the threshold for significance.

## ■ ASSOCIATED CONTENT

### Supporting Information

The Supporting Information is available free of charge at https://pubs.acs.org/doi/10.1021/acsomega.2c05833.

Pictures of *C. wilfordii* adventitious roots (ARs) affected by MS salt concentration (Figure S1); analysis results of conduritol F (Figure S2), hydroxyacetophenones (Figure S3, Table S1), phenolic compounds (Figure S4, Table S2), low-molecular-weight hydrophilic compounds (Figure S5, Table S3), and fatty acids (Figure S6, Table S4); scheme of the adopted process for *C. wilfordii* adventitious root (AR) proliferation (Figure S7) (PDF)

## ■ AUTHOR INFORMATION


### Corresponding Author

**Young-Min Ham** − *Biodiversity Research Institute, Jeju 63608, Republic of Korea;* orcid.org/0000-0001-9887-3552; Phone: +82-64-720-2830; Email: hijel@jejutp.or.kr; Fax: +82-64-720-2801

### Authors

**Hyejin Hyeon** − *Biodiversity Research Institute, Jeju 63608, Republic of Korea;* orcid.org/0000-0002-8680-0548

**Eun Bi Jang** − *Biodiversity Research Institute, Jeju 63608, Republic of Korea*

**Weon-Jong Yoon** − *Biodiversity Research Institute, Jeju 63608, Republic of Korea*

**Jong-Du Lee** − *Biodiversity Research Institute, Jeju 63608, Republic of Korea*

**Ho Bong Hyun** − *Biodiversity Research Institute, Jeju 63608, Republic of Korea*

**Yong-Hwan Jung** − *Biodiversity Research Institute, Jeju 63608, Republic of Korea*

**Jung Min** − *Jeju Chyeonnyeonyakcho Farming Co., Jeju, Jeju 63052, Republic of Korea*

Complete contact information is available at: https://pubs.acs.org/10.1021/acsomega.2c05833

### Author Contributions

#H.H. and E.B.J. contributed equally to this work as first authors.


### Author Contributions

All authors have read and agreed to the published version of the manuscript. Conceptualization: Y.-H.J. and J.M.; resources: E.B.J., J.-D.L., Y.-H.J., and J.M.; methodology: H.H., E.B.J., J.-D.L., and H.B.H.; data curation, formal analysis, investigation, validation, visualization: H.H. and E.B.J; writing − original draft, writing − review & editing: H.H., E.B.J, W.-J.Y., and Y.-M.H.; project administration, supervision: Y.-M.H.

### Notes

The authors declare no competing financial interest.

## ■ ACKNOWLEDGMENTS

This work did not receive funding from any private, public, or not-for-profit agency organization.

## ■ REFERENCES


(1) Hwang, I.-S.; Yoo, J.-H.; Seong, E.-S.; Lee, J.-G.; Kim, H.-Y.; Kim, N.-J.; Lee, J.-D.; Ham, J.-K.; Ahn, Y.-S.; Kim, N.-Y.; Yu, C.-Y. The Effect of Temperature and Seed Soaking on Germination in *Cynanchum wilfordii* (Maxim.) Hemsl. *Korean J. Med. Crop Sci* **2012**, *20*, 136−139.

(2) Youn, J. S.; Ham, Y. M.; Yoon, W.-J.; Choi, H.-C.; Lee, J. E.; Cho, B.; Kim, J. Y. *Cynanchum wilfordii* etanolic extract controls blood cholesterol: A double-blind, randomized, placebo-controlled, parallel trial. *Nutrients* **2019**, *11*, 836.

(3) Jeong, S.; Lee, S.; Choi, W. J.; Sohn, U. D.; Kim, W. The effect of polyphenols isolated from *Cynanchi wilfordii* Radix with anti-inflammatory, antioxidant, and anti-bacterial activity. *Korean J. Physiol. Pharmacol.* **2015**, *19*, 151−158.

(4) Lee, H.; Kim, M. H.; Choi, Y. Y.; Hong, J.; Yang, W. M. Effects of *Cynanchum wilfordii* on osteoporosis with inhibition of bone resorption and induction of bone formation. *Mol. Med. Rep.* **2017**, *17*, 3758−3762.

(5) Lee, M. K.; Yeo, H.; Kim, J.; Kim, Y. C. Protection of rat hepatocytes exposed to CCl4 in-vitro by cynandione A, a biacetophenone from *Cynanchum wilfordii*. *J. Pharm. Pharmacol.* **2000**, *52*, 341−345.

(6) Jiang, Y.; Choi, H. G.; Li, Y.; Park, Y. M.; Lee, J.-H.; Kim, D. H.; Lee, J.-H.; Son, J. K.; Na, M.; Lee, S. H. Chemical constituents of *Cynanchum wilfordii* and the chemotaxonomy of two species of the family Asclepiadacease, *C. wilfordii* and *C. auriculatum*. *Arch. Pharmacal Res.* **2011**, *34*, 2021−2027.

(7) Kim, S. H.; Kim, W. C.; Kim, H. H.; Heo, K. Cytogenetical Study of *Cynanchum wilfordii* and *Cynanchum auriculatum* using Fluorescence *In Situ* Hybridization (FISH). *Korean J. Med. Crop Sci.* **2020**, *28*, 325−330.
(8) Li, Y.; Piao, D.; Zhang, H.; Woo, M.-H.; Lee, J.-H.; Moon, D.-C.; Lee, S.-H.; Chang, H. W.; Son, J. K. Quality assessment and discrimination of the roots of *Cynanchum auriculatum* and *Cynanchum wilfordii* by HPLC−UV analysis. *Arch. Pharmacal Res.* **2013**, *36*, 335−344.
(9) Isah, T.; Umar, S.; Mujib, A.; Sharma, M. P.; Rajasekharan, P. E.; Zafar, N.; Frukh, A. Secondary metabolism of pharmaceuticals in the plant in vitro cultures: strategies, approaches, and limitations to achieving higher yield. *Plant Cell, Tissue Organ Cult.* **2018**, *132*, 239−265.
(10) Ahn, M. S.; So, E. J.; Jie, E. Y.; Choi, S. Y.; Park, S. U.; Moon, B. C.; Kang, Y. M.; Min, S. R.; Kim, S. W. Metabolic comparison between standard medicinal parts and their adventitious roots of *Cynanchum wilfordii* (Maxim.) Hemsl. using FT-IR spectroscopy after IBA and elicitor treatment. *J. Plant Biotechnol.* **2018**, *45*, 250−256.
(11) Murthy, H. N.; Dandin, V. S.; Paek, K.-Y. Tools for biotechnological production of useful phytochemicals from adventitious root cultures. *Phytochem. Rev.* **2016**, *15*, 129−145.
(12) Ho, T.-T.; Lee, K.-J.; Lee, J.-D.; Bhushan, S.; Paek, K.-Y.; Park, S.-Y. Adventitious root culture of *Polygonum multiflorum* for phenolic compounds and its pilot-scale production in 500 L-tank. *Plant Cell, Tissue Organ Cult.* **2017**, *130*, 167−181.
(13) Lee, K.-J.; Park, Y.; Kim, J.-Y.; Jeong, T.-K.; Yun, K.-S.; Paek, K.-Y.; Park, S.-Y. Production of biomass and bioactive compounds from adventitious root cultures of *Polygonum multiflorum* using air-lift bioreactors. *J. Plant Biotechnol.* **2015**, *42*, 34−42.
(14) Yue, W.; Ming, Q.-L.; Lin, B.; Rahman, K.; Zheng, C.-J.; Han, T.; Qin, L. Medicinal plant cell suspension cultures: pharmaceutical applications and high-yielding strategies for the desired secondary metabolites. *Crit. Rev. Biotechnol.* **2016**, *36*, 215−232.
(15) Strzemski, M.; Dresler, S.; Sowa, I.; Czubacka, A.; Agacka-Mołdoch, M.; Płachno, B. J.; Granica, S.; Feldo, M.; Wójciak-Kosior, M. The impact of different cultivation systems on the content of selected secondary metabolites and antioxidant activity of *Carlina acaulis* plant material. *Molecules* **2019**, *25*, 146.
(16) Zuo, S.-M.; Yu, H.-D.; Zhang, W.; Zhong, Q.; Chen, W.; Chen, W.; Yun, Y.-H.; Chen, H. Comparative metabolomic analysis of *Dendrobium officinale* under different cultivation substrates. *Metabolites* **2020**, *10*, 325.
(17) Yun, D.-Y.; Kang, Y.-G.; Lee, E. J.; Kim, D.; Kim, E.-H.; Hong, Y.-S. Metabolomics study for exploring metabolic perturbations in soybean adventitious roots by fluorescent light irradiation. *Appl. Biol. Chem.* **2021**, *64*, 26.
(18) Feng, Z.; Ding, C.; Li, W.; Wang, D.; Cui, D. Applications of metabolomics in the research of soybean plant under abiotic stress. *Food Chem.* **2020**, *310*, 125914.
(19) Chinou, I. Primary and secondary metabolites and their biological activity. In *Thin Layer Chromatography in Phytochemistry*; 1st ed.; Chromatographic Science Series; Vol. *99*; CRC Press: Florida, 2008; pp. 59−75, DOI: 10.1201/9781420046786
(20) Murashige, T.; Skoog, F. A revised medium for rapid growth and bio assays with tobacco tissue cultures. *Physiol. Plant.* **1962**, *15*, 473−497.
(21) Murthy, H. N.; Kim, Y.-S.; Park, S.-Y.; Paek, K.-Y. Biotechnological production of caffeic acid derivatives from cell and organ cultures of *Echinacea* species. *Appl. Microbiol. Biotechnol.* **2014**, *98*, 7707−7717.
(22) Yin, S.; Zhang, Y.; Gao, W.; Wang, J.; Man, S.; Liu, H. Effects of nitrogen source and phosphate concentration on biomass and metabolites accumulation in adventitious root culture of *Glycyrrhiza uralensis* Fisch. *Acta Physiol. Plant.* **2014**, *36*, 915−921.
(23) Lee, E.-J.; Paek, K.-Y. Enhanced productivity of biomass and bioactive compounds through bioreactor cultures of *Eleutherococcus koreanum* Nakai adventitious roots affected by medium salt strength. *Ind. Crops Prod.* **2012**, *36*, 460−465.
(24) Sun, H. D.; Gao, Y.; An, X. L.; Jiang, X. L.; Piao, X. C.; Jin, M. Y.; Lian, M. L. Optimization of the culture medium of adventitious root culture to produce the flavonoids and the triterpenoids of *Actinidia arguta* by using an orthogonal design process. *Plant Cell, Tissue Organ Cult.* **2021**, *144*, 545−554.
(25) Zhang, J.; Gao, W.-Y.; Wang, J.; Li, X.-L. Effects of sucrose concentration and exogenous hormones on growth and periplocin accumulation in adventitious roots of *Periploca sepium* Bunge. *Acta Physiol. Plant.* **2012**, *34*, 1345−1351.
(26) Chan, L. K.; Dewi, P. R.; Boey, R. L. Effect of plant growth regulators on regeneration of plantlets from bud cultures of *Cymbopogon nardus* L. and the detection of essential oils from the *in vitro* plantlets. *J. Plant Biol.* **2005**, *48*, 142−146.
(27) Cui, X.-H.; Chakrabarty, D.; Lee, E.-J.; Paek, K.-Y. Production of adventitious roots and secondary metabolites by *Hypericum perforatum* L. in a bioreactor. *Bioresour. Technol.* **2010**, *101*, 4708−4716.
(28) Davies, P.J. The plant hormone concept: Concentration, sensitivity and transport. In *Plant hormones*; 2nd ed.; Davies, P. J., Ed.; Vol. *1*; Springer: Dordrecht, 1995; pp. 13−38, DOI: 10.1007/978-94-011-0473-9_2
(29) Manuhara, Y. S. W.; Kristanti, A. N.; Utami, E. S. W.; Yachya, A. Effect of sucrose and potassium nitrate on biomass and saponin content of *Talinum paniculatum* Gaertn. hairy root in balloon-type bubble bioreactor. *Asian Pac. J. Trop. Biomed.* **2015**, *5*, 1027−1032.
(30) Bahmani, R.; Karami, O.; Gholami, M. Influence of carbon sources and their concentrations on rooting and hyperhydricity of apple rootstock MM. 106. *World Applied Sciences Journal*; 2009, *6*, 1513−1517. Available in: idosi.org/wasj/wasj6(11)/9.pdf (accessed 2022-10-21).
(31) Ahn, J.-K.; Lee, W.-Y.; Park, S.-Y. Effect of nitrogen source on the cell growth and production of secondary metabolites in bioreactor cultures of *Eleutherococcus senticosus*. *Korean J. Plant Biotechnol.* **2003**, *30*, 301−305.
(32) Yaseen, M.; Ahmad, T.; Sablok, G.; Standardi, A.; Hafiz, I. A. Review: role of carbon sources for in vitro plant growth and development. *Mol. Biol. Rep.* **2013**, *40*, 2837−2849.
(33) Lai, Z.; Fiehn, O. Mass spectral fragmentation of trimethylsilylated small molecules. *Mass Spectrom. Rev.* **2018**, *37*, 245−257.
(34) Kim, J. K.; Choi, S. R.; Lee, J.; Park, S.-Y.; Song, S. Y.; Na, J.; Kim, S. W.; Kim, S.-J.; Nou, I.-S.; Lee, Y. H.; Park, S.-U.; Kim, H. Metabolic differentiation of diamondback moth (*Plutella xylostella* (L.)) resistance in cabbage (*Brassica oleracea* L. ssp. *capitata*). *J. Agric. Food Chem.* **2013**, *61*, 11222−11230.
(35) Zhang, X.; Shan, L.; Huang, H.; Yang, X.; Liang, X.; Xing, A.; Huang, H.; Liu, X.; Su, J.; Zhang, W. Rapid identification of acetophenones in two *Cynanchum* species using liquid chromatography−electrospray ionization tandem mass spectrometry. *J. Pharm. Biomed. Anal.* **2009**, *49*, 715−725.
(36) Wang, L.; Cai, F.; Zhao, W.; Tian, J.; Kong, D.; Sun, X.; Liu, Q.; Chen, Y.; An, Y.; Wang, F.; Liu, X.; Wu, Y.; Zhou, H. *Cynanchum auriculatum* Royle ex Wight., *Cynanchum bungei* Decne. and *Cynanchum wilfordii* (Maxim.) Hemsl.: Current Research and Prospects. *Molecules* **2021**, *26*, 7065.
(37) Erb, M.; Kliebenstein, D. J. Plant secondary metabolites as defenses, regulators, and primary metabolites: the blurred functional trichotomy. *Plant Physiol.* **2020**, *184*, 39−52.
(38) Worley, B.; Powers, R. Multivariate analysis in metabolomics. *Curr. Metabolomics* **2013**, *1*, 92−107.
(39) Khanam, M. N.; Anis, M.; Javed, S. B.; Mottaghipisheh, J.; Csupor, D. Adventitious Root Culture—An Alternative Strategy for Secondary Metabolite Production: A Review. *Agronomy* **2022**, *12*, 1178.
(40) Rahmat, E.; Kang, Y. Adventitious root culture for secondary metabolite production in medicinal plants: a review. *J. Plant Biotechnol.* **2019**, *46*, 143−157.
(41) Gromski, P. S.; Muhamadali, H.; Ellis, D. I.; Xu, Y.; Correa, E.; Turner, M. L.; Goodacre, R. A tutorial review: Metabolomics and


https://doi.org/10.1021/acsomega.2c05833
*ACS Omega* 2022, 7, 46756−46768

partial least squares-discriminant analysis—a marriage of convenience or a shotgun wedding. *Anal. Chim. Acta* **2015**, *879*, 10−23.
(42) Triba, M. N.; Le Moyec, L.; Amathieu, R.; Goossens, C.; Bouchemal, N.; Nahon, P.; Rutledge, D. N.; Savarin, P. PLS/OPLS models in metabolomics: the impact of permutation of dataset rows on the K-fold cross-validation quality parameters. *Mol. BioSyst.* **2015**, *11*, 13−19.
(43) Jäger, T.; Holandino, C.; Melo, M. N. d. O.; Peñaloza, E. M. C.; Oliveira, A. P.; Garrett, R.; Glauser, G.; Grazi, M.; Ramm, H.; Urech, K.; Baumgartner, S. Metabolomics by UHPLC-Q-TOF Reveals Host Tree-Dependent Phytochemical Variation in *Viscum album* L. *Plants* **2021**, *10*, 1726.
(44) Hyeon, H.; Xu, J. L.; Kim, J. K.; Choi, Y. Comparative metabolic profiling of cultivated and wild black soybeans reveals distinct metabolic alterations associated with their domestication. *Food Res. Int.* **2020**, *134*, 109290.
(45) Galili, G. The aspartate-family pathway of plants: linking production of essential amino acids with energy and stress regulation. *Plant Signaling Behav.* **2011**, *6*, 192−195.
(46) Yang, D.-S.; Zhang, J.; Li, M.-X.; Shi, L.-X. Metabolomics analysis reveals the salt-tolerant mechanism in *Glycine soja*. *J. Plant Growth Regul.* **2017**, *36*, 460−471.
(47) Kim, T. J.; Kim, S. Y.; Park, Y. J.; Lim, S.-H.; Ha, S.-H.; Park, S. U.; Lee, B.; Kim, J. K. Metabolite profiling reveals distinct modulation of complex metabolic networks in non-pigmented, black, and red rice (*Oryza sativa* L.) Cultivars. *Metabolites* **2021**, *11*, 367.
(48) Zhu, D.; Si, H.; Zhang, P.; Geng, A.; Zhang, W.; Yang, B.; Qian, W.-J.; Gabriel, M.; Sun, J. Genomics and biochemistry investigation on the metabolic pathway of milled wood and alkali lignin-derived aromatic metabolites of *Comamonas serinivorans* SP-35. *Biotechnol. Biofuels* **2018**, *11*, 338.
(49) O'Brien, J. A.; Daudi, A.; Butt, V. S.; Paul Bolwell, G. Reactive oxygen species and their role in plant defence and cell wall metabolism. *Planta* **2012**, *236*, 765−779.
(50) He, M.; Ding, N.-Z. Plant unsaturated fatty acids: multiple roles in stress response. *Front. Plant Sci.* **2020**, *11*, 562785.
(51) Lei, A.; Chen, H.; Shen, G.; Hu, Z.; Chen, L.; Wang, J. Expression of fatty acid synthesis genes and fatty acid accumulation in *Haematococcus pluvialis* under different stressors. *Biotechnol. Biofuels* **2012**, *5*, 18.
(52) Nakabayashi, R.; Saito, K. Integrated metabolomics for abiotic stress responses in plants. *Curr. Opin. Plant Biol.* **2015**, *24*, 10−16.
(53) Zhang, L.; Li, X.; Ma, B.; Gao, Q.; Du, H.; Han, Y.; Li, Y.; Cao, Y.; Qi, M.; Zhu, Y.; Lu, H.; Ma, M.; Liu, L.; Zhou, J.; Nan, C.; Qin, Y.; Wang, J.; Cui, L.; Liu, H.; Liang, C.; Qiao, Z. The tartary buckwheat genome provides insights into rutin biosynthesis and abiotic stress tolerance. *Mol. Plant* **2017**, *10*, 1224−1237.
(54) Nakabayashi, R.; Yonekura-Sakakibara, K.; Urano, K.; Suzuki, M.; Yamada, Y.; Nishizawa, T.; Matsuda, F.; Kojima, M.; Sakakibara, H.; Shinozaki, K.; Michael, A. J.; Tohge, T.; Yamazaki, M.; Saito, K. Enhancement of oxidative and drought tolerance in Arabidopsis by overaccumulation of antioxidant flavonoids. *Plant J.* **2014**, *77*, 367−379.
(55) Yeshi, K.; Crayn, D.; Ritmejerytė, E.; Wangchuk, P. Plant secondary metabolites produced in response to abiotic stresses has potential application in pharmaceutical product development. *Molecules* **2022**, *27*, 313.
(56) Sharma, A.; Shahzad, B.; Rehman, A.; Bhardwaj, R.; Landi, M.; Zheng, B. Response of phenylpropanoid pathway and the role of polyphenols in plants under abiotic stress. *Molecules* **2019**, *24*, 2452.
(57) Obata, T.; Fernie, A. R. The use of metabolomics to dissect plant responses to abiotic stresses. *Cell. Mol. Life Sci.* **2012**, *69*, 3225−3243.
(58) Egert, A.; Keller, F.; Peters, S. Abiotic stress-induced accumulation of raffinose in Arabidopsis leaves is mediated by a single raffinose synthase (RS5, At5g40390). *BMC Plant Biol.* **2013**, *13*, 218.
(59) Khan, N.; Ali, S.; Zandi, P.; Mehmood, A.; Ullah, S.; Ikram, M.; Ismail, M. A. S.; Babar, M. A. Role of sugars, amino acids and organic acids in improving plant abiotic stress tolerance. *Pak. J. Bot.* **2020**, *52*, 355−363.
(60) Napoleão, T. A.; Soares, G.; Vital, C. E.; Bastos, C.; Castro, R.; Loureiro, M. E.; Giordano, A. Methyl jasmonate and salicylic acid are able to modify cell wall but only salicylic acid alters biomass digestibility in the model grass *Brachypodium distachyon*. *Plant Sci.* **2017**, *263*, 46−54.
(61) Kim, T. J.; Hyeon, H.; Park, N. I.; Yi, T. G.; Lim, S.-H.; Park, S.-Y.; Ha, S.-H.; Kim, J. K. A high-throughput platform for interpretation of metabolite profile data from pepper (*Capsicum*) fruits of 13 phenotypes associated with different fruit maturity states. *Food Chem.* **2020**, *331*, 127286.
(62) Lei, S.; Rossi, S.; Huang, B. Metabolic and Physiological Regulation of Aspartic Acid-Mediated Enhancement of Heat Stress Tolerance in Perennial Ryegrass. *Plants* **2022**, *11*, 199.
(63) Khodakovskaya, M.; McAvoy, R.; Peters, J.; Wu, H.; Li, Y. Enhanced cold tolerance in transgenic tobacco expressing a chloroplast $\omega$-3 fatty acid desaturase gene under the control of a cold-inducible promoter. *Planta* **2006**, *223*, 1090−1100.
(64) Yuan, S.; Wu, X.; Liu, Z.; Luo, H.; Huang, R. Abiotic stresses and phytohormones regulate expression of FAD2 gene in *Arabidopsis thaliana*. *J. Integr. Agric.* **2012**, *11*, 62−72.
(65) Jemal, F.; Zarrouk, M.; Ghorbal, M. H. Effect of cadmium on lipid composition of pepper. *Biochem. Soc. Trans.* **2000**, *28*, 907−910.
(66) Palomino-Schätzlein, M.; Montaño, M. C.; Escrig, P. V.; Boira, H.; Corma, A.; Pineda-Lucena, A.; Primo, J.; Cabedo, N. Identification of Bioactive Compounds in Polar and Nonpolar Extracts of *Araujia sericifera*. *Planta Med. Int. Open* **2017**, *4*, e93−e103.
(67) Kim, T. J.; Park, J. G.; Ahn, S. K.; Kim, K. W.; Choi, J.; Kim, H. Y.; Ha, S.-H.; Seo, W. D.; Kim, J. K. Discrimination of adzuki bean (*Vigna angularis*) geographical origin by targeted and non-targeted metabolite profiling with gas chromatography time-of-flight mass spectrometry. *Metabolites* **2020**, *10*, 112.
(68) Park, C. H.; Yeo, H. J.; Lim, H.-S.; Hyeon, H.; Kim, J. K.; Park, S. U. Gene Expression and Metabolic Analyses of Nontransgenic and *AtPAP* 1 Transgenic Tobacco Infected with *Potato Virus X* (PVX). *J. Agric. Food Chem.* **2022**, *70*, 5838−5848.
(69) Balci, M.; Sütbeyaz, Y.; Seçen, H. Conduritols and related compounds. *Tetrahedron* **1990**, *46*, 3715−3742.


https://doi.org/10.1021/acsomega.2c05833
*ACS Omega* 2022, 7, 46756−46768